Supporting Information

Microscopic Visualization of $NiFeO_x$ and NiO_x Cocatalyst Effects on Charge Carrier Dynamics of $BiVO_4$ Photoanodes

Yuki Nakatsukasa,[1] Haruka Nobuoka and Kenji Katayama[1*]

1 Department of Applied Chemistry, Chuo University, Tokyo 112-8551, Japan;

*Corresponding authors:

K. Katayama, Phone: +81-3-3817-1913, E-mail: kkata.33g@g.chuo-u.ac.jp

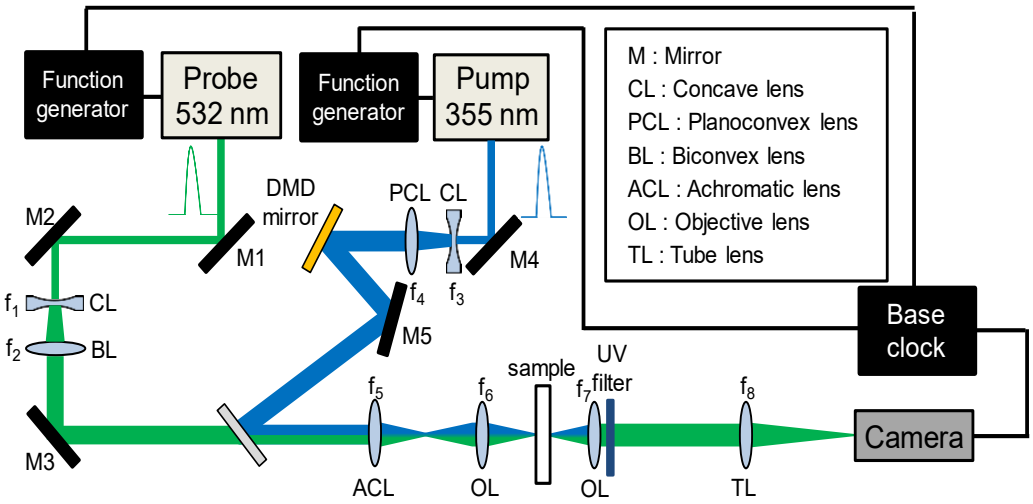

Figure S1 The schematic overview of the optical setup of the patterned-illumination time-resolved phase microscopy (PI-PM) is shown. Pattern illumination was achieved using a digital micromirror device (DMD) (Light Crafter 4500, Texas Instruments). The pump light, reflected off the DMD, created variable light patterns that mirrored those designed on a computer. These patterns were then projected onto the sample, reduced to 1/14th of their original size, through a combination of a lens (f = 100 mm) and an objective lens (LUCPLELN20X, Olympus). The pulsed illumination was synchronized with the pump light via a dichroic mirror and directed onto the sample. The light passing through the sample was captured using another objective lens (LUCPLFLN20x, Olympus) and a tube lens (TTL180-A, Thorlabs), and imaged onto a CMOS camera (MV1-D1024E-160, Photon Focus) with a sensor size of 10.9 x 10.9 mm (1024 x 1024 pixels), focusing on a central strip (200 x 1024 pixels). The diameter of the sample area illuminated by the pump pulse was 0.5 mm. Adjusting the delay between the pump and probe pulses allowed for the capture of a sequence of images, with the temporal resolution being determined by the pulse widths of the pump and probe lights, which ranged from 3 to 5 ns. The pump light was generated by the third harmonic of a Nd:YAG pulse laser (pulse width: 3-5 ns, wavelength: 355 nm) from GAIA, Rayture Systems, while the probe light came from the second harmonic of another Nd:YAG pulse laser (pulse width: 5 ns, wavelength: 532 nm) from the same supplier. The timing of the pulses was meticulously regulated by two function generators (WF1968, NF) synchronized to a base clock (DF1906, NF), each controlling the flash lamp and Q-switch timing with a precision of 100 ps. The intensities of the pump and probe lights were 0.8 mJ/pulse and 0.02 mJ/pulse, respectively.

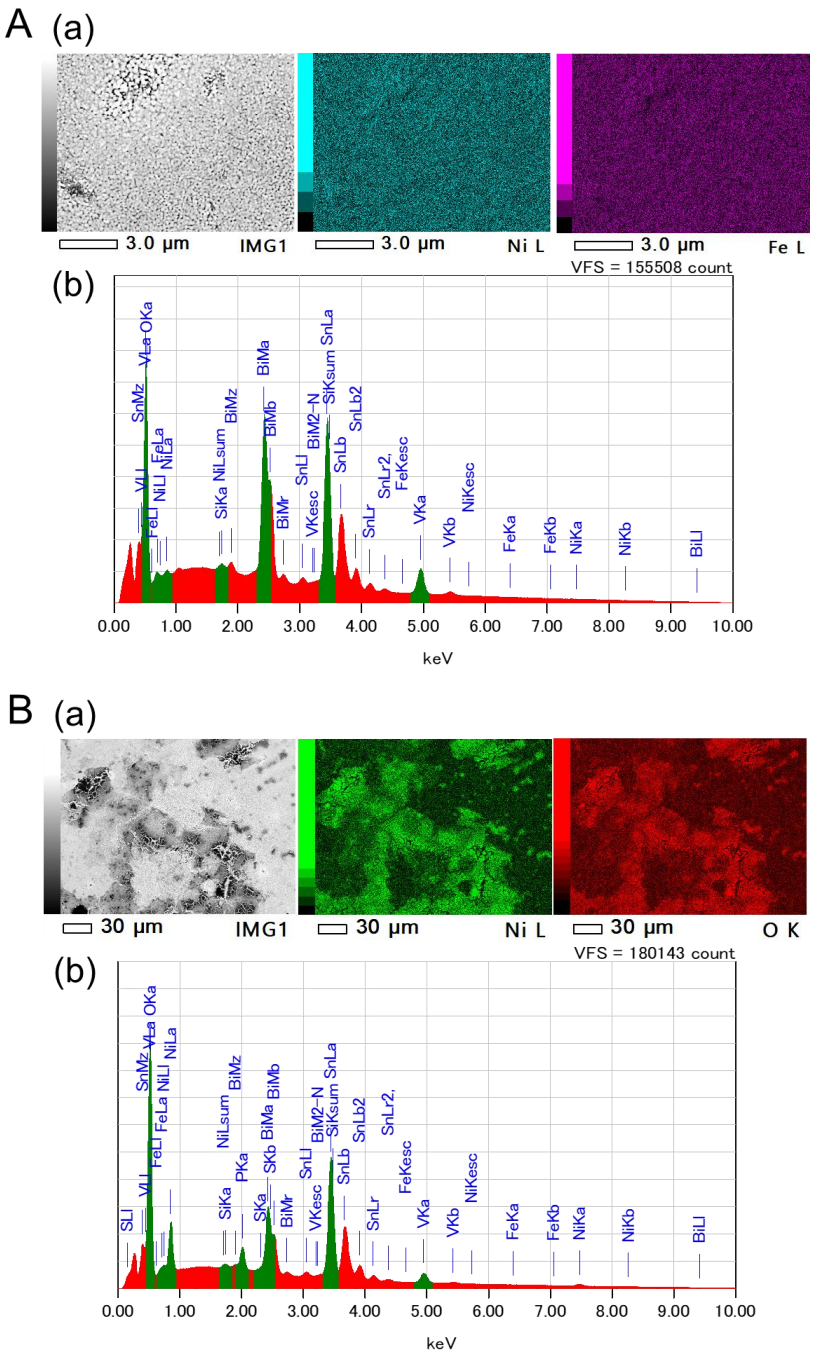

Figure S2 Energy Dispersive X-ray Spectroscopy (EDS) results for (A) $BiVO_4/NiFeO_x$ and (B) $BiVO_4/NiO_x$. (a) corresponds to the microscopic image and mapping results of the elements, and obtained EDS spectrum was shown in (b). In $BiVO_4/NiFeO_x$ observation, the maximum magnification was employed due to the charge-up constraints, but no specific distribution of the elements was confirmed. In the case of $BiVO_4/NiO_x$, a boundary region of the NiO_x overlayer and an exposed $BiVO_4$ region was chosen for analysis.

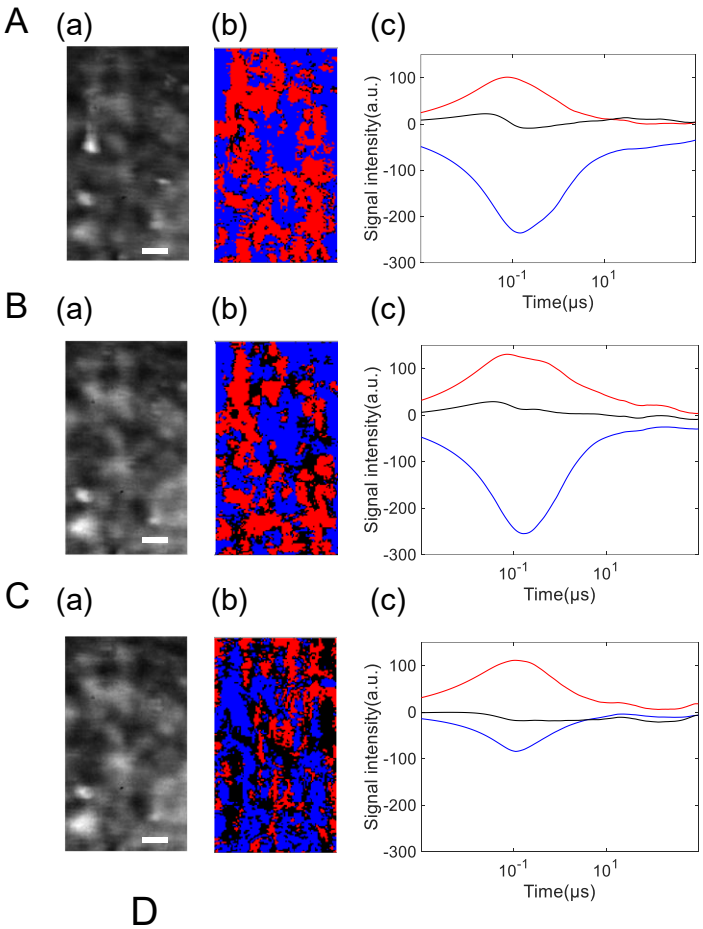

D

Solvent	Category	Ratio [%]	Rise [ns]	Decay [μs]
ACN	1 (Red)	44	11 ± 1	0.6 ± 0.1
	3 (Blue)	47	23 ± 2	1.5 ± 0.1
	5 (Black)	9	-	-
EtOH	1 (Red)	34	10 ± 1	1.5 ± 0.1
	3 (Blue)	41	25 ± 2	1.1 ± 0.1
	5 (Black)	14	-	-
NB/ EtOH	1 (Red)	26	13 ± 1	0.8 ± 0.1
	3 (Blue)	16	23 ± 2	0.6 ± 0.1
	5 (Black)	58	-	-

Figure S3 Clustering analyses of the charge carrier responses of a bare $BiVO_4$ in (A) ACN, (B) EtOH, and (C) NB/EtOH in region 2 in Figure 5(a). (a) correspond to a microscopic image, and the corresponding categorized map is shown in (b), and The scale bar corresponds to 10 μm. The averaged responses for the categorized responses are shown in (c). The ratios of categories and the rise/decay times for the categories are shown in (D).

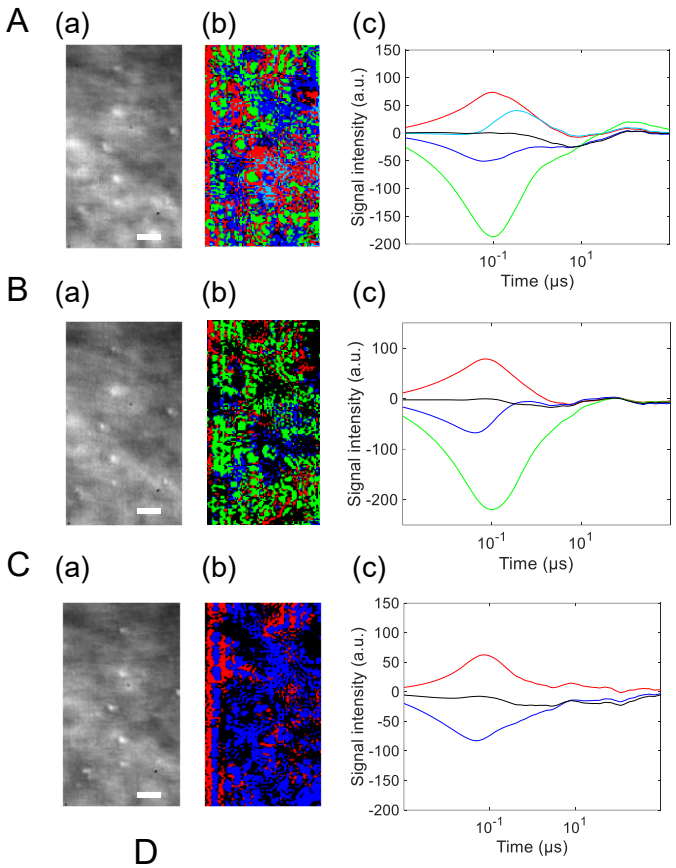

D

Solvent	Category	Ratio [%]	Rise [ns]	Decay [μs]
ACN	1 (Red)	29	17 ± 1	0.3 ± 0.1
	2 (Cyan)	5	103 ± 7	1.4 ± 0.1
	3 (Blue)	29	11 ± 1	0.4 ± 0.1
	4 (Green)	25	15 ± 1	0.5 ± 0.1
	5 (Black)	12	-	-
EtOH	1 (Red)	9	13 ± 1	0.3 ± 0.1
	2 (Cyan)	0	-	-
	3 (Blue)	9	8 ± 1	0.1 ± 0.1
	4 (Green)	29	15 ± 1	0.6 ± 0.1
	5 (Black)	53	-	-
NB/ EtOH	1 (Red)	13	16 ± 1	0.3 ± 0.1
	2 (Cyan)	0	-	-
	3 (Blue)	39	7 ± 1	0.5 ± 0.1
	4 (Green)	0	-	-
	5 (Black)	48	-	-

Figure S4 Clustering analyses of the charge carrier responses of a $BiVO_4/NiFeO_x$ photoanode in (A) ACN, (B) EtOH, and (C) NB/EtOH in region 1 in Figure 5(b). (a) correspond to a microscopic image, and the corresponding categorized map is shown in (b), and The scale bar corresponds to 10 mm. The averaged responses for the categorized responses are shown in (c). The ratios of categories and the rise/decay times for the categories are shown in (D).

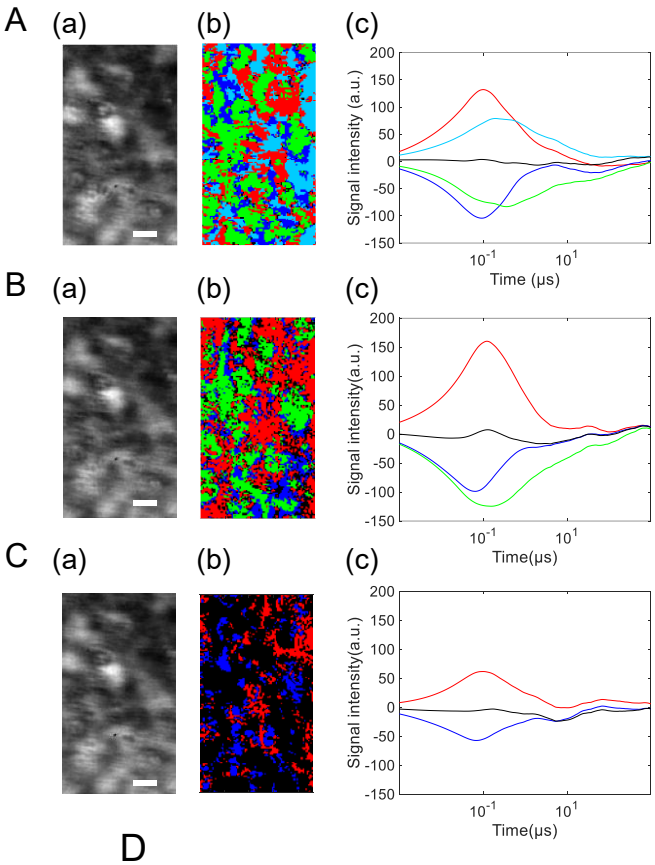

D

Solvent	Category	Ratio [%]	Rise [ns]	Decay [μs]
ACN	1 (Red)	27	16 ± 1	0.6 ± 0.1
	2 (Cyan)	22	27 ± 2	2.7 ± 0.3
	3 (Blue)	16	15 ± 1	0.4 ± 0.1
	4 (Green)	32	21 ± 2	5.0 ± 0.4
	5 (Black)	2	-	-
EtOH	1 (Red)	37	21 ± 1	0.7 ± 0.1
	2 (Cyan)	0	-	-
	3 (Blue)	16	8 ± 1	0.3 ± 0.1
	4 (Green)	29	13 ± 1	1.9 ± 0.1
	5 (Black)	19	-	-
NB/ EtOH	1 (Red)	14	17 ± 1	0.5 ± 0.1
	2 (Cyan)	0	-	-
	3 (Blue)	13	10 ± 1	0.4 ± 0.1
	4 (Green)	0	-	-
	5 (Black)	74	-	-

Figure S5 Clustering analyses of the charge carrier responses of a $BiVO_4/NiO_x$ photoanode in (A) ACN, (B) EtOH, and (C) NB/EtOH in region 1 in Figure 5(c). (a) correspond to a microscopic image, and the corresponding categorized map is shown in (b), and The scale bar corresponds to 10 mm. The averaged responses for the categorized responses are shown in (c). The ratios of categories and the rise/decay times for the categories are shown in (D).